

**THE SIZES OF 1720 MHZ OH MASERS: VLBA AND MERLIN
OBSERVATIONS OF THE SUPERNOVA REMNANTS W 44
AND W 28**

M. J. Claussen, W. M. Goss, D. A. Frail, & K. Desai

National Radio Astronomy Observatory (NRAO) Array Operations Center, P.O. Box O,
Socorro, New Mexico 87801, USA

Received _____; accepted _____

To be published in *The Astrophysical Journal*

ABSTRACT

We have used the NRAO Very Long Baseline Array (VLBA) to image OH(1720 MHz) masers in the supernova remnants W28 and W44 at a resolution of 40 mas. We also used MERLIN to observe the same OH(1720 MHz) masers in W44 at a resolution of 290×165 mas. All the masers are resolved by these VLBA and MERLIN observations. The measured sizes range from 50 to 180 mas and yield brightness temperature estimates from $0.3\text{--}20 \times 10^8$ K. We investigate whether these measured angular sizes are intrinsic and hence originate as a result of the physical conditions in the supernova remnant shock, or whether they are scatter broadened sizes produced by the turbulent ionized gas along the line of sight. While the current data on the temporal and angular broadening of pulsars, masers and extragalactic sources toward W44 and W28 can be understood in terms of scattering, we cannot rule out that these large sizes are intrinsic. Recent theoretical modeling by Lockett et al. suggests that the physical parameters in the shocked region are indicative of densities and OH abundances which lead to estimates of sizes as large as what we measure. If the sizes and structure are intrinsic, then the OH(1720 MHz) masers may be more like the OH(1612 MHz) masers in circumstellar shells than OH masers associated with H II regions. At two locations in W28 we observe the classical S-shapes in the Stokes V profiles caused by Zeeman splitting and use it to infer magnetic fields of order 2 milliGauss.

Subject headings: masers — ISM: supernova remnants — scattering

1. Introduction

The 1720.53 MHz line from the hydroxyl radical (OH) was conclusively shown to be associated with the supernova remnant (SNR) W 28 by Frail, Goss & Slysh (1994). Since then several surveys have been made toward other Galactic SNRs (Frail et al. 1996, Yusef-Zadeh et al. 1996, Green et al. 1997, Koralesky et al. 1998), clearly establishing that the OH(1720 MHz) line toward masers is a new class of OH maser, distinct from those in star-forming regions and evolved stars. Follow-up work (Claussen et al. 1997, Frail & Mitchell 1998, Wardle, Yusef-Zadeh & Geballe 1998) supports the hypothesis that the OH(1720 MHz) masers originate in C-type shocks, transverse to the line-of-sight, being driven into adjacent molecular clouds by the expanding SNR. The measured densities, temperatures and magnetic fields from these studies are consistent with collisional excitation of the OH by the H₂ molecules in the post-shock gas (Elitzur 1976, Pavlakis & Kylafis 1996, Lockett, Gauthier, & Elitzur 1999).

Claussen et al. (1997) imaged the masers toward the SNRs W 28 and W 44 and reported finding numerous maser features distributed across these SNRs. At their arcsecond resolution, some features were unresolved (“spots”) while other features appeared to be resolved with measured angular sizes ranging from 0.25” to 2.5”. These measured sizes of the masers could, of course, be spots that appeared spatially blended due to insufficient angular resolution. Alternatively, the resolved features could be spots whose apparent sizes reflect scattering by interstellar turbulence along the line of sight (angular broadening). Many masers are known whose apparent sizes are dominated by angular broadening (e.g., Diamond et al. 1998; Frail et al. 1994); most such masers are seen with similar sizes and elongations as noted by Claussen et al. (1997).

The current study was undertaken primarily to address the question of whether the measured size of the masers is due to scattering or to multiple maser components. In order

to reach a definite conclusion on this question, we must investigate both the intrinsic size of the masers and the possible effects of interstellar scattering.

The OH(1720 MHz) masers are quite rare in the interstellar medium as compared to main-line masers, and even more so toward late-type stars where the other satellite line at 1612 MHz is the dominant maser transition. So published sizes of OH(1720 MHz) masers, which necessitate the use of VLBI techniques are also very rare. Forster et al. (1982) found upper limits of 20 mas to the sizes of OH(1720 MHz) masers toward the H II region NGC 7538, while Mashedder et al. (1994) reported that the W3(OH) 1720 MHz masers are unresolved with sizes <1.2 mas. These measurements may not even be applicable in the case of supernova remnants where the physical conditions and pumping mechanisms could be very different from that in star-forming regions. A recent study of the pumping of the 1720 MHz masers toward supernova remnants (Lockett et al. 1999) finds tight constraints on the physical conditions needed for their production (temperature in the range 50 — 125 K, molecular hydrogen density $\sim 10^5$ cm $^{-3}$, and OH column densities of order 10^{16} cm $^{-2}$.) An upper limit for the size of the maser spots is the thickness of the shocked region over which such conditions exist. This thickness is estimated to be about 3×10^{15} cm. At the distance (3 kpc) of both W 44 and W 28, this corresponds to an angular size of about 60 mas.

The effects of interstellar scattering on the sizes of masers in W 28 and W 44 can be constrained by observations of nearby (in projection) pulsars and extragalactic sources. Interstellar scattering of an extragalactic source results in angular broadening while interstellar scattering of pulsars results in pulse broadening, an increase in the apparent width of a pulsar's average pulse profile beyond its intrinsic width. The degree of angular broadening for the masers and the extragalactic source and the degree of pulse broadening for the pulsar all depend in different ways upon the relative geometry of the observer,

scattering material, and sources. Measurements of these three scattering effects can constrain the distribution of the scattering material and can be used to estimate, for example, the unscattered sizes of the masers.

In this paper, we present VLBI observations of several bright OH(1720 MHz) masers in W 28 and W 44 using the VLBA of the NRAO. The large extent of the SNRs and associated maser emission (tens of arcminutes) precluded observations of all the OH masers for these remnants. In addition, we have used the MERLIN telescope of the Nuffield Radio Astronomy Laboratory at Jodrell Bank to observe the OH masers in W 44 with intermediate angular resolution between that of the VLBA and the VLA. We present the results of these observations and discuss their impact on the question of the masers’ intrinsic size vs. broadening due to interstellar scattering.

2. Observations and Data Reduction

2.1. VLBA Observations

The 1720 MHz transition of the ground-state OH molecule was observed with the VLBA (Napier et al. 1994) on 09 May 1997 toward one $\sim 25'$ field in each of the two supernova remnants W 28 and W 44. Table 1 lists the position of the pointing center for both sources. These positions were chosen to encompass both the “OH E” and “OH F” 1720 MHz masers in W 28 and the “OH E” masers in W 44, following the nomenclature of Claussen et al. (1997). A single antenna of the VLA was also used in conjunction with the antennas of the VLBA in order to provide short projected baselines (~ 60 km).

The data were recorded with a 62.5 kHz bandwidth centered at velocities of 44.0 km s^{-1} and 10.0 km s^{-1} (LSR) for W 44 and W 28, respectively. Both right and left circular polarizations were recorded with 2-bit sampling. The data were correlated with the

NRAO VLBA correlator to provide 128 spectral channels for each polarization averaged every 4.1 seconds. All four polarization correlations were performed. This correlator mode provided a channel spacing of 0.09 km s^{-1} per spectral channel. The velocity resolution is slightly large than this ($\sim 0.11 \text{ km s}^{-1}$) due to the spectral weighting function applied.

In order to provide manageable dataset sizes, the correlator averaging time was the limiting factor for the field of view. For averaging times of 4.1 seconds, the fringe-rate window for the longest baselines of the VLBA provides a field of view of approximately $24''$. Thus for both SNRs we made two correlation passes near positions of strong OH(1720 MHz) masers in the primary field of view. Table 2 provides the positions of the two correlation positions for both remnants, and the peak flux density in the VLA **A** configuration observations (Claussen et al. 1997).

Data reduction was performed using standard software contained in the NRAO AIPS package. Delays were measured via observations of nearby continuum sources (1748–253 for W 28, and 1904+013 for W 44) by performing fringe fitting. Bandpass calibration was determined using total-power observations of the strong sources 1921–293 and 1611+343. Residual fringe rates were determined by fringe fitting on a single strong spectral channel. For W 28, amplitude calibration was accomplished by fitting the bandpass-corrected, total-power, on-source spectra of each antenna in the array to a template total-power, on-source spectrum observed with a sensitive antenna (at the Mauna Kea, HI station) at a high elevation angle. The absolute amplitude calibration determined by this method is accurate to about 10%. For W 44, the amplitude calibration was determined by using known antenna gains (provided by NRAO staff) and system temperatures measured during the observations (so-called *a priori* amplitude calibration). This procedure was carried out for the W 44 data because the signal-to-noise ratio in the total-power spectra of the OH maser line was not high enough to attempt the template-fitting method. The absolute

amplitude calibration determined by the *a priori* method is accurate to about 15%. Even on the strongest spectral channels, no correlated signal was detected on the longer baselines (typically from one of the southwest locations to Saint Croix, VI; Hancock, NH; and Mauna Kea, HI), and so data to these stations were automatically deleted.

The spectral channel with the greatest flux density was then used in an iterative self-calibration mapping procedure. These self-calibration solutions were then applied to all spectral channels. The rms noise (≈ 100 mJy beam $^{-1}$) in these images is close to the expected theoretical noise limit. Images were then made of all spectral channels with maser emission. Naturally weighted maps for each velocity channel were then produced using the AIPS task IMAGR. The resultant synthesized beam was about 40×15 mas at a position angle of 0° for W 28, and about 40×30 mas at a position angle of -10° for W 44.

2.2. MERLIN Observations

The MERLIN radio telescope was used on 12 April 1998 to observe the position listed in Table 1 for W 44 in the 1720 MHz transition of OH. Seven telescopes were used, including the 76-m Lovell telescope, the Mark II, the 32-m telescope at Cambridge, and the 25-m telescopes at Tabley, Darnhall, Knockin, and Defford. Both right and left-hand polarization was observed, and the correlator produced 512 spectral channels over a bandwidth of 500 kHz, for a channel spacing of 0.18 km s^{-1} . The field of view for the MERLIN observations included both the W 44 “E” and “F” sources (Claussen et al. 1997). The synthesized beam from the MERLIN observations was 290×165 mas at a position angle of 25° .

Initial phase and amplitude calibration was performed by MERLIN staff at the University of Manchester. Bandpass calibration was determined from observations of 3C 84, and phase calibration was determined from interleaved observations of 1904+013. The

absolute amplitude calibration was determined by observations of 3C 286 on the shortest baselines.

Similar to the VLBA reduction, AIPS was then used to apply self-calibration solutions, based on iterative self-calibration imaging carried out on the strongest spectral channel. The rms noise obtained after applying the self-calibration to a single channel was about 30 mJy beam⁻¹, also close to the theoretical noise limit.

3. Results

3.1. W 28 Masers

Figure 1 shows a contour image of the OH(1720 MHz) emission at 11.3 km s⁻¹, and Stokes *I* spectra at two emission peaks. This emission corresponds to feature F 39 in the nomenclature of Claussen et al. (1997) (see their Table 2). The peak flux density in the image is 6.1 Jy beam⁻¹ with a total flux of ~ 70 Jy, in close agreement with the peak flux density (73 Jy beam⁻¹) at this position in the VLA **A** configuration maps. The OH(1720 MHz) emission is clearly resolved at this resolution. Several emission peaks can be seen. The size of the feature marked **B** in Figure 1, determined by Gaussian fitting, is 75×34 mas, at a position angle of 9° . Thus the peak brightness temperature is $\sim 2 \times 10^9$ K. Other emission peaks in the contour image of Figure 1 have similar spectral profiles, differing primarily in their peak flux density. In addition to the masers shown in Figure 1, there is an additional maser emission peak ~ 500 mas to the northeast, at a velocity of 9.6 km s⁻¹. Figure 2 shows a contour image of the peak velocity channel in this region and Stokes *I* spectra of two emission peaks. Again, the emission is quite extended (size ~ 60 mas) compared with the beam. The two peaks **C** and **D** in the emission correspond to brightness temperatures of 1×10^9 and 8×10^8 K, respectively.

For the positions marked **A** and **B** in Figure 1, we have determined the Stokes parameters I and V . Assuming the V profile is due to the Zeeman effect, and that the splitting is small compared to the intrinsic (Doppler) line width, the Stokes V profile is proportional to the frequency derivative of the Stokes I profile. A fit of the V profile to the derivative of the I profile yields a measurement of the line-of-sight magnetic field (see Claussen et al. 1997 for further discussion). Figure 3 shows the result of this fit for the two positions marked in Figure 1. The estimate of the line-of-sight magnetic field (~ 2 milliGauss) is larger by a factor of ~ 10 than estimates based on the VLA observations. However, toward this specific position, Claussen et al. (1997) were unable to estimate the line-of-sight magnetic field because the spectra were quite complex and did not show a clear signature (the classical S-shape in Stokes V) of Zeeman splitting.

This relation used to derive the line-of-sight magnetic field is valid only for thermal absorption and emission lines. Nedoluha & Watson (1992) conclude that the standard thermal relationship used here is a valid approximation of the line-of-sight field strength for observations of water masers, if they are not strongly saturated, despite the complications of the maser radiative transfer. Elitzur (1996, 1998) has derived a general polarization solution for maser emission and arbitrary Zeeman splitting. According to this solution, Elitzur (1998) concludes that masers require smaller fields to produce the same amount of circular polarization as thermal emission. Thus the estimate of the magnetic field given above may be overestimated by as much as factors of 2–4.

At the other correlated position in W 28 (W 28 E), we did not detect OH emission. Based on the VLA observations, we expected that there should be several features detectable by the VLBA. Some of the flux densities measured in the VLA observations are 24 Jy/beam (E 30), 12.5 Jy/beam (E 31), and 10 Jy/beam (E 24). E 24 was *unresolved* with the VLA. If these non-detections are due to emission that is smooth, we can calculate a lower limit to

the size of the emission features, based on the rms noise that we measured on the shortest projected baseline in the VLBA observations. Assuming a source size that is a circular Gaussian function, a maximum visibility of 0.1 (for E 24, for example) on the shortest baseline (~ 60 km), the lower limit must be about 400 mas. For E 30, the visibility must be correspondingly lower and thus the size must be larger than about 500 mas.

3.2. W 44 Masers

The OH(1720 MHz) masers observed with MERLIN are shown in Figures 4 and 5. Figure 4 is a contour plot of the peak maser emission from the E 11 source along with the OH spectrum of the peak emission. The peak occurs at a velocity of 44.2 km s^{-1} . The stronger of the two features in the contour image has a peak flux density of 3.3 Jy beam^{-1} , and is slightly resolved with a fitted Gaussian size of 165×57 mas at a position angle of 147° . The total flux density over the emission region is about 6.1 Jy, which is comparable to the peak flux density measured with the VLA. The brightness temperature for this feature is 1.3×10^8 K. We convolved the MERLIN map of the E 11 source with the VLA **A** configuration beam, and then made a Gaussian fit to the resulting image. The peak of the convolved image was 5.0 Jy beam^{-1} with a fitted size of 715×250 mas at a position angle of 166° . This is comparable with the VLA observations which obtained a peak flux density of 6.6 Jy beam^{-1} , and a fitted size of 890×180 at a position angle of 137° .

Figure 5 shows the OH(1720 MHz) maser emission from the W 44 F 24 source which peaks at a velocity of 46.9 km s^{-1} , with a peak flux density of 1.5 Jy beam^{-1} . The OH spectrum at the emission peak is also shown. The total flux density in the emission region is about 4.2 Jy, only about half of the VLA observed peak flux density.

Figure 6 shows a contour plot of the VLBA image of the E 11 source. This maser

source is unresolved at the resolution of the VLBA (40×30 mas). The peak flux density is 1.2 Jy beam^{-1} , and thus a lower limit to the brightness temperature is $8 \times 10^8 \text{ K}$. This source is the core of the brightest MERLIN source shown in Figure 4. If a single Gaussian component with a large size were responsible for the difference in flux density between the VLBA and MERLIN measurements, then, based on the shortest projected spacing of the VLBA and the measured noise, the size of such feature would have to be larger than 270 mas. This is inconsistent with the MERLIN measurement. Thus we conclude that the 2.1 Jy of missing flux density must be in a few components whose peaks are each weaker than about 0.4 Jy beam^{-1} .

4. The OH Maser Sizes: Scattering Disks or Physical Size?

Table 3 summarizes the measured components and the estimated brightness temperatures of the OH(1720 MHz) masers in both W28 and W44. The VLBA and MERLIN observations clearly resolve the masers seen by Claussen et al. (1997) into multiple components. Typical angular sizes in both SNRs are 50 to 100 mas with aspect ratios of order 2.5:1. While these measurements have shown that the Claussen et al. (1997) maser sizes were an artifact of the low resolution used, a major question remains: “are these compact and resolved features the true size of the masers or are they due to interstellar scattering?”. The observations and results of the present study cannot distinguish between these two options. This is due mainly to our ignorance of what the intrinsic sizes might be. In what follows we will interpret the results of these observations as they apply to both intrinsic structure and that due to scattering, and suggest further observational tests that should help to distinguish between these two possibilities.

4.1. Scattering Interpretation

If the maser sizes in W 44 and W 28 are dominated by scattering, other nearby (in projection) objects such as pulsars and extragalactic sources can also be affected. Pulse broadening and angular broadening depend in different ways upon the distribution of scattering material along the line of sight; additionally, angular broadening of an extragalactic source seen through the turbulence in our Galaxy’s ISM is sensitive only to the strength of the turbulence, not to its distribution along the line of sight. The relative distances of the masers and nearby pulsars along with the distribution of scattering material can all be constrained using measurements of angular and pulse broadening.

Adopting a distance of 3 kpc for both W 28 and W 44 , the models of Cordes et al. (1991) and Taylor & Cordes (1993) predict angularly broadened sizes for the OH masers of order 1–3 mas. These angular broadening estimates are well below the sizes given in Table 3 but it should be noted that the angular broadening is underestimated for lines-of-sight subject to enhanced scattering. Examples of lines-of-sight with enhanced scattering include the Galactic Center region (van Langevelde et al. 1992), the Cygnus region (Fey, Spangler & Cordes 1991), and towards 1849+005 (Fey, Spangler & Cordes 1991). We discuss separately the implications of our maser size measurements for the scattering towards W 28 and W 44.

4.1.1. Scattering in the Direction of W 28

The W 28 SNR and its associated masers lie at a distance of approximately 3 kpc (e.g., Kaspi et al. 1993; Frail, Kulkarni, & Vasisht 1993) in the direction $(l, b) = (6.8, -0.06)$. The 60,000 year old pulsar PSR B1578–23 also lies in the same direction but is located outside the SNR, a few arcminutes to the north of its bright continuum edge. An extragalactic source, 1758–231, lies within two arcminutes of this pulsar. Frail et al. (1993),

using observations of the pulsar and the neighboring extragalactic source, argued in favor of the association of the pulsar and the SNR. Kaspi et al. (1993) disagreed, suggesting that the pulsar was much further away. The discussion of Frail et al. was based upon a pulse broadening measurement of 70 milliseconds at 1 GHz for PSR B1758–23 (Kaspi et al. 1993) and upon an upper limit of 1 arcsecond to the size of the extragalactic source 1758–231. Here we review the implications of our measurements of the 60 mas maser size as it pertains to this disagreement.

Under the usual assumption that masers and the extragalactic source are scattered by a turbulence confined to a single thin screen, angular broadening measurements completely constrain the location of the screen. The two angular broadening sizes are related to the location of the screen by

$$d_s/d_m = 1 - \theta_m/\theta_e,$$

where θ_m and θ_e are the angular broadening sizes of the masers and the extragalactic source and d_m and d_s are the observer distances to the masers and the screen, respectively. If the masers and the extragalactic source have sizes of $\theta_e = 1''$ and $\theta_m = 0.06''$, respectively, then for a maser distance of $d_m = 3$ kpc, the scattering screen lies at $d_s = 2.8$ kpc. Note that the screen distance decreases if θ_m/θ_e increases.

The pulse broadening of PSR1758–231 and the angular broadening of 1758–231 provide a general constraint on the location of the pulsar. Frail et al. (1993) assumed a distance of 3 kpc for PSR B1758–23 and combined the pulse broadening of PSR B1758–23 with the angular broadening of 1758–231 to constrain f_p , the ratio of the observer-screen distance to the screen-pulsar distance, to values between 0.3 and 3.4. A more general constraint on the location of the pulsar can be obtained if the equations presented by Frail et al. are combined without assuming a distance to the pulsar to produce

$$\theta_e = \frac{0.42}{\sqrt{d_p/3}} \left(\sqrt{f_p} + \frac{1}{\sqrt{f_p}} \right),$$

where θ_e is the angular size of the extragalactic source in arcseconds, and d_p is the distance from the observer to the pulsar in kpc. It is easy to show that this implies that the distance to the pulsar is given by

$$d_p = 2.12/\theta_e^2,$$

if the screen is halfway to the pulsar and is further otherwise. In particular, if the measured extragalactic source size is smaller than 0.84 arcseconds, the pulsar cannot be associated with the W 28 SNR.

4.1.2. *Scattering in the Direction of W 44*

The W 44 SNR and its associated masers lie at a distance of approximately 3 kpc (Radhakrishnan et al. 1972) in the direction $(l, b) = (34.7, -0.4)$. The association of pulsar PSR B1853+01 with W 44 is well established based on ages, dispersion measure distance, and positional coincidence (Wolszczan, Cordes, & Dewey 1991). Assuming a 3 kpc distance to PSR B1853+01, the Taylor & Cordes model predicts 30 microseconds of pulse broadening and 1 mas of angular broadening. Because the Taylor & Cordes model prediction of 92 mas severely underestimates the observed angular broadening size of 378 mas for 1849+005, an extragalactic source situated only 3.7 degrees away from W 44, we consider the possibility that the observed 100 mas OH maser sizes are due to angular broadening. The observational limit to the pulse broadening is of order 1 millisecond.

Lines-of-sight with enhanced scattering are believed to intersect a clumped component of scattering material in the interstellar medium. All lines-of-sight passing within 30 arcminutes of the Galactic Center are known to be heavily scattered (van Langevelde et al. 1992; Lazio & Cordes 1998). The scattering material has been constrained to lie within 50 parsecs of the Galactic Center. At a distance of 8.5 kpc, a clump of size 30 arcminutes corresponds to enhanced scattering in a region of about 40 pc. Similar clump

sizes have been proposed for scattering towards other lines-of-sight (e.g., Dennison et al. 1984).

Because the OH masers in W 44 and PSR B1853+01 both lie at 3 kpc, the distance d_s (in kpc) to an assumed scattering screen can be derived from the pulsar size formula presented by Frail et al. :

$$d_s = \frac{3}{1 + \theta_m^2/2.52\tau},$$

where θ_m is measured in arcseconds and τ , the pulse broadening, is measured in seconds. If the angular broadening size for OH masers in W 44 is assumed to be 80 mas and the pulse broadening of order 0.5 milliseconds, a clump of enhanced scattering would need to be placed only 0.5 kpc away. At this distance, a 40 pc clump would subtend an angle of about 4 degrees and could also intercept the line of sight towards 1849+005. Since the line-of-sight towards 1849+005 is the second most heavily angularly broadened line of sight known, it is reasonable to suggest that other, neighboring, lines-of-sight should also be heavily scattered — as is the case for the Galactic Center direction. The observed sizes of OH masers in W 44, if dominated by angular broadening, have sizes consistent with the scattering of 1849+005. This hypothesis predicts that other lines-of-sight close to 1849+005 should also be heavily scattered. In addition, improved better measurements of the pulse-broadening towards PSR B1853+01 could help to prove or disprove this suggestion.

4.2. Intrinsic Structure of the Masers

If the structure that is observed in the OH(1720MHz) masers toward W 44 and especially W 28 are due to variations in emission intrinsic to the maser, then this data is the first demonstration of structure in 1720 MHz OH maser emission. The pumping requirements of these OH (1720 MHz) masers, modeled by Lockett et al. (1999), strongly suggests an OH column density of 10^{16} cm^{-2} with molecular hydrogen density $\sim 10^5 \text{ cm}^{-3}$.

This requires a linear dimension of $\frac{10^{11}}{x_{OH}}$ cm, where x_{OH} is the OH abundance. According to Lockett et al. (1999), the highest OH abundance expected in C-shocks is $\sim 2 \times 10^{-5}$, so the expected thickness of the OH emitting region is about 5×10^{15} cm, similar to the maser sizes we observe.

We could conclude that these masers appear to be similar to the stellar OH(1612 MHz) masers. The OH(1612 MHz) masers in circumstellar shells show a large range of size scales: 40 — 1000 mas, as demonstrated by Bowers et al. (1990). Both main-line and 1720 MHz OH found in the interstellar medium have been shown to be very compact and with little structure (e.g., Reid et al. 1980; Forster et al. 1982; Mashedier et al. 1994). Bowers et al. (1990) suggest that the OH(1612 MHz) maser structure is determined by a combination of density and velocity effects; our 1720 MHz observations could be indicative of a similar situation.

A good test of whether or not the OH(1720 MHz) emission is really due to intrinsic structure would be a high-resolution observation of the OH(1720 MHz) emission toward a nearby SNR in the anti-center direction (to minimize possible scattering effects). A good candidate for this test observation would be the SNR IC 443. It lies at a Galactic longitude $\approx 189^\circ$, and is only 1.5 kpc distant. If a measurement of the size of the OH(1720 MHz) masers in IC 443 showed the masers to be smaller than those in W 28 or W 44, then a good argument for scattering of the masers in W 28 and W 44 could be made. If the sizes of the masers in IC 443 were similar in size or larger than those in W 28 or W 44, then the sizes of the masers in all three of the SNR would likely be intrinsic.

5. The OH Maser Polarization in W 28: Magnetic Fields

The measurement of the line-of-sight magnetic field of about 2 milliGauss toward the region of strong maser emission in W 28 is stronger than the more widespread measurements reported by Claussen et al. (1997) toward the SNR by about a factor of 10. This measurement is closer to that reported by Yusef-Zadeh et al. (1996, 1998) for magnetic fields in the Galactic Center. It is interesting to note that the strongest field strength we measure is also in the region of strongest maser emission. This may be a selection effect, since our observations were limited to only a few maser regions. Since both the current observations and the VLA observations of V profiles show the classical S shapes of the Zeeman effect, we are confident that both sets of measurements are good estimates of the line-of-sight magnetic field.

In this small region, the magnetic pressure must be 100 times the pressure estimated by Claussen et al. (1997), or about 2×10^{-7} dyn cm $^{-2}$. Thus the magnetic pressure is very much larger than the thermal gas pressure of 6×10^{-10} dyn cm $^{-2}$ estimated from hot X-ray gas in the interior of the remnants (Rho et al. 1996), and so the magnetic field is likely the dominant factor in the structure of the shock. As discussed by Lockett et al. (1999) and Draine, Roberge, and Dalgarno (1983), the larger magnetic field estimated here is further strong evidence for a C-type shock in the OH maser region.

6. Conclusions

We have used the VLBA and MERLIN to observe some of the OH(1720 MHz) masers toward the two supernova remnants W 44 and W 28 at resolutions of 40 mas. We have resolved the masers in both SNRs. The range of observed sizes are 50–180 mas, and the derived apparent brightness temperatures are in the range 0.3– 20×10^8 K. Based on the

present data, it is unclear if the observed structure of the masers is due to interstellar scattering or to intrinsic structure.

If the OH(1720 MHz) structure is due to intrinsic maser emission, then we suggest that the OH(1720 MHz) masers in SNR may be similar to the OH(1612 MHz) maser emission from circumstellar shells. A possible test of whether or not the size and structures observed are intrinsic or due to scattering would be a high angular resolution observation of the remnant IC 443.

If the sizes measured are considered to be dominated by the angular broadening effects of interstellar scattering, conclusions can be drawn about the location of the scattering material. In the case of W 28, the scattering material along the line of sight is most likely situated within ~ 100 pc of the masers. Also, we would conclude that pulsar PSR B1758–23 is definitely *not* associated with the SNR. In the case of W 44, we suggest that a 40 pc clump of enhanced scattering material located 500 pc from the Sun could explain the observed maser sizes as well as the scattering of 1849+005. This suggestion could be tested by searching for other heavily scattered sources within ≈ 4 degrees of 1849+005 and by improved pulse broadening measurements of the pulsar PSR B1853+01.

Finally, we measure a magnetic field in a small region of the SNR W 28 ($\sim 2 \times 10^{15}$ cm), which is a factor of about 10 higher than that which was measured using the VLA. The magnetic field clearly dominates the shock structure, and is further evidence for a C-type shock in the OH maser region.

The National Radio Astronomy Observatory is a facility of the National Science Foundation, operated under cooperative agreement by Associated Universities, Inc. MERLIN is a UK national facility operated by the University of Manchester on behalf of PPARC. We thank Peter Wilkinson for granting us time on MERLIN from the Director's

discretion, Peter Thomasson for his invaluable assistance in scheduling MERLIN, and Anita Richards for performing the initial phase and amplitude calibration for the MERLIN data. Finally, we thank the referee, Moshe Elitzur, for useful comments and discussions which have improved the paper.

REFERENCES

- Claussen, M. J, Frail, D. A., Goss, W. M., & Gaume, R. A. 1997, *ApJ*, 489, 143
- Cordes, J. M., Weisberg, J. M., Frail, D. A., Spangler, S. R., & Ryan, M. 1991, *Nature*, 354, 121
- Dennison, B., Thomas, M., Booth, R. S., Brown, R. L., Broderick, J. J., & Condon, J. J. 1984, *A&A*, 135, 199
- Diamond, P. J., Martinson, A., Dennison, B. Booth, R. S., & Winnberg, A. 1988, in *Radio Wave Scattering in the Interstellar Medium*, ed. J. Cordes, B. J. Rickett, & D. C. Backer (New York: AIP), 195
- Draine, B. T., Roberge, W. G., and Dalgarno, A. 1983, *ApJ*, 264, 485
- Elitzur, M. 1976, *ApJ*, 203, 124
- Elitzur, M. 1996, *ApJ*, 457, 415
- Elitzur, M. 1998, *ApJ*, 504, 390
- Fey, A. L., Spangler, S. R., & Cordes, J. M. 1991, *ApJ*, 372, 132
- Forster, J. R., Graham, D., Goss, W. M., & Booth, R. S. 1982, *MNRAS*, 201, 7P.
- Frail, D. A., Kulkarni, S. R., & Vasisht, G. 1993, *Nature*, 365, 136
- Frail, D. A., Goss, W. M., & Slysh, V. I. 1994, *ApJ*, 424, L111
- Frail, D. A., Goss, W. M., Reynoso, E. M., Giacani, E. B., & Green, A. J. 1996, *AJ*, 111, 1651
- Frail, D. A. & Mitchell, G. F. 1998, *ApJ*, 508, 690
- Frail, D. A., Diamond, P. J., Cordes, J. M., & Van Langevelde, H. J. *ApJ*, 1994, 427, L43
- Giacani, E. B., Dubner, G. M., Kassim, N. E., Frail, D. A., Goss, W. M., Winkler, P. F., & Williams, B. F. 1997, *AJ*, 113, 1379

- Green, A. J., Frail, D. A., Goss, W. M., & Otrupcek, R. 1997, *AJ*, 114, 2058
- Gwinn, C. R., Moran, J. M., Reid, M. J., & Schneps, M. H. 1988, *ApJ*, 330, 817
- Kaspi, V. M., Lyne, A. G., Manchester, R. N., Johnston, S., D’Amico, N., & Shemar, S. L. 1993, *ApJ*, 409, L57
- Lazio, T. J. W., & Cordes, J. M. 1998, *ApJ*, 505, 715
- Koralesky, B., Frail, D. A., Goss, W. M., Claussen, M. J., & Green, A. J. 1998, *AJ*, 116, 323
- Lockett, P., Gauthier, E., & Elitzur, M. 1999, *ApJ*, 511, in press.
- Manchester, R. N., D’Amico, N., & Tuohy, I. R. 1985, *MNRAS*, 212, 975
- Mashedier, M. R. W., Field, D., Gray, M. D., Migenes, V., Cohen, R. J., & Booth, R. S. 1994, *A&A*, 281, 871
- Moran, J. M., et al. 1973, *ApJ*, 185, 535
- Napier, P. J., Bagri, D. S., Clark, B. G., Rogers, A. E. E., Romney, J. D., Thompson, A. R., & Walker, R. C. 1994, *Proc. IEEE*, 82, 658
- Nedoluha, G. E., & Watson, W. D. 1992, *ApJ*, 384, 185
- Pavlakis, K. G., & Kylafis, N. D. 1996a, *ApJ*, 467, 300
- Radhakrishnan, V., Goss, W. M., Murray, J. D., & Brooks, J. W. 1972, *ApJS*, 24, 49
- Reid, M. J., Haschick, A. D., Burke, B. F., Moran, J. M., Johnston, K. J., & Swenson, G. W., Jr. 1980, *ApJ*, 239, 89
- Rho, J. -H., Petre, R., Pisarski, R., Jones, L. R. 1996, in “Röntgenstrahlung from the Universe” eds. H. U. Zimmermann, J. E. Trümper, and H. Yorke, *MPE Report* 263, p. 273
- Spangler, S. R., Fey, A. L., & Cordes, J. M. 1987, *ApJ*, 322, 939
- Taylor, J. H. & Cordes, J. M. 1993, *ApJ*, 411, 674

van Dishoeck, E. F., Jansen, D. J., & Phillips, T. G. 1993, *A&A*, 279, 541

van Langevelde, H. J., Frail, D. A., Cordes, J. M. & Diamond, P. J. 1992, *ApJ*, 396, 686

Wolszczan, A., Cordes, J. M., & Dewey, R. J. 1991, *ApJ*, 372, L99

Wardle, M., Yusef-Zadeh, F., & Geballe, T. R., submitted to *ApJ*

Yusef-Zadeh, F., Roberts, D. A., Goss, W. M., Frail, D. A., & Green, A. J. 1996, *ApJ*, 466,
L25

Yusef-Zadeh, F., Roberts, D. A., Goss, W. M., Frail, D. A., & Green, A. J. 1998, *ApJ*, in
press.

Table 1: Pointing Positions of VLBA Observations

Source	RA (J2000)	Decl. (J2000)
W 28	$18^h 01^m 51^s.473$	$-23^\circ 17'49''.64$
W 44	$18^h 56^m 29^s.099$	$+01^\circ 29'43''.36$

Table 2: VLBA Correlation Positions and VLA Peak Flux Densities

Source	RA (J2000)	Decl. (J2000)	Peak Flux Density (Jy beam ⁻¹)
W 28 OH E	$18^h 01^m 51^s.198$	$-23^\circ 17'40''.64$	24.4
W 28 OH F	$18^h 01^m 52^s.706$	$-23^\circ 19'24''.64$	73.0
W 44 OH E	$18^h 56^m 26^s.665$	$+01^\circ 29'43''.36$	6.6
W 44 OH F	$18^h 56^m 36^s.627$	$+01^\circ 26'35''.89$	8.9

Table 3: Measured Properties of 1720 MHz OH Masers in W 28 and W 44

Source	Major Axis (mas)	Minor Axis (mas)	P.A. (deg)	Peak Flux Density (Jy beam ⁻¹)	T _B (10 ⁸ K)
W 28 F 39 A	105	34	20	5.5	10
W 28 F 39 B	75	34	9	6.1	20
W 28 F 39 C	68	39	21	3.2	8
W 28 F 39 D	58	31	24	3.1	10
W 44 F 24	240	135	121	1.5	0.3
W 44 E 11 (MERLIN)	165	57	147	3.3	2
W 44 E 11 (VLBA)	<40	<30	—	1.2	>6

Fig. 1.— A VLBA contour image of the OH(1720 MHz) maser emission from feature F 39 in W 28, following nomenclature of Claussen et al. (1997). The contours are plotted at 0.3, 0.53, 0.93, 1.63, 2.86, and 5.00 Jy beam⁻¹. The insets show Stokes *I* spectra taken at the peaks marked **A** and **B** by crosses.

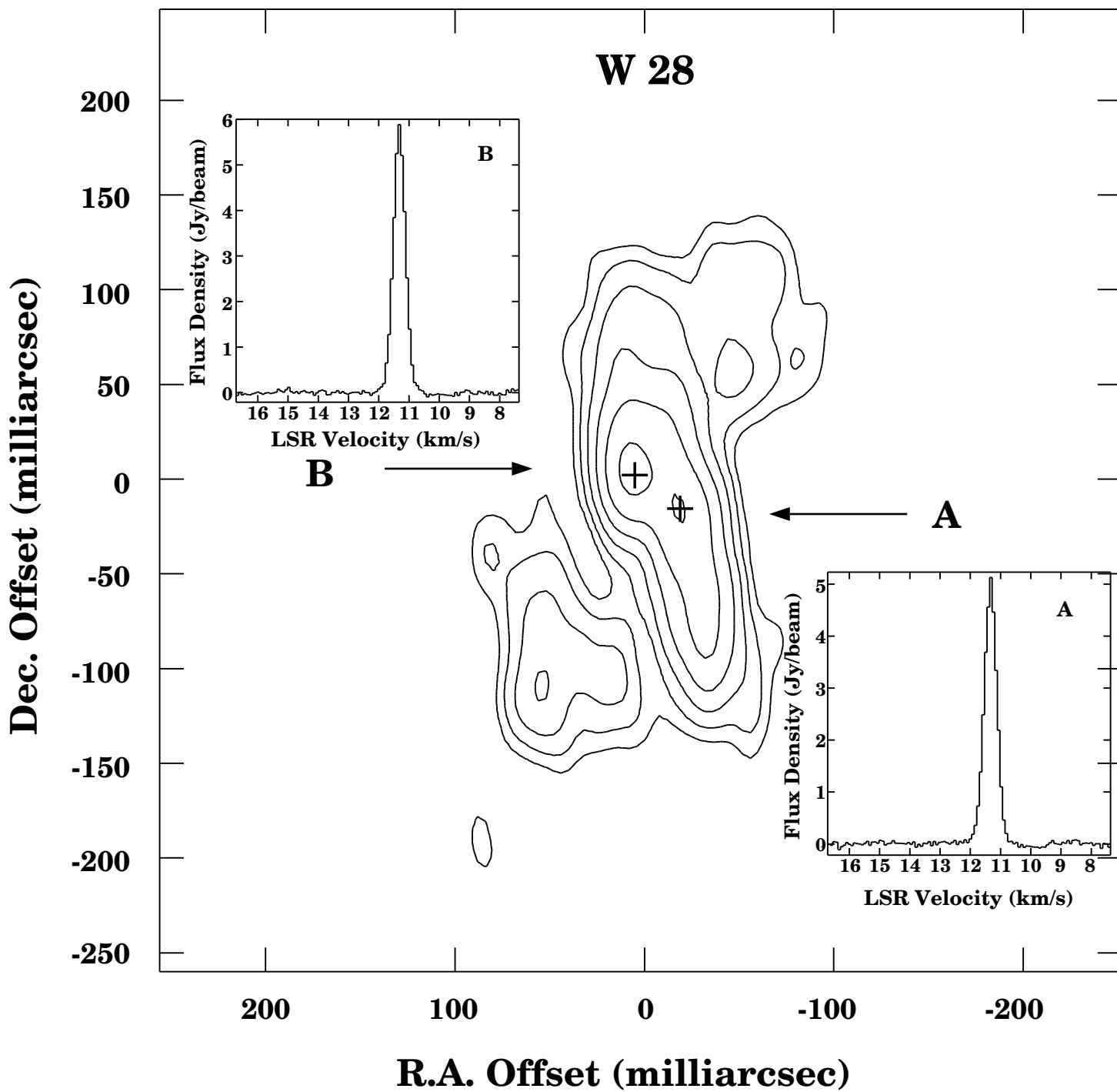
Fig. 2.— A VLBA contour image of the OH(1720 MHz) maser emission in W 28, about 500 mas to the northeast of the emission shown in Figure 1. The contours are plotted at the same levels as in Figure 1. The insets show Stokes *I* spectra taken at the emission peaks marked **C** and **D** by crosses.

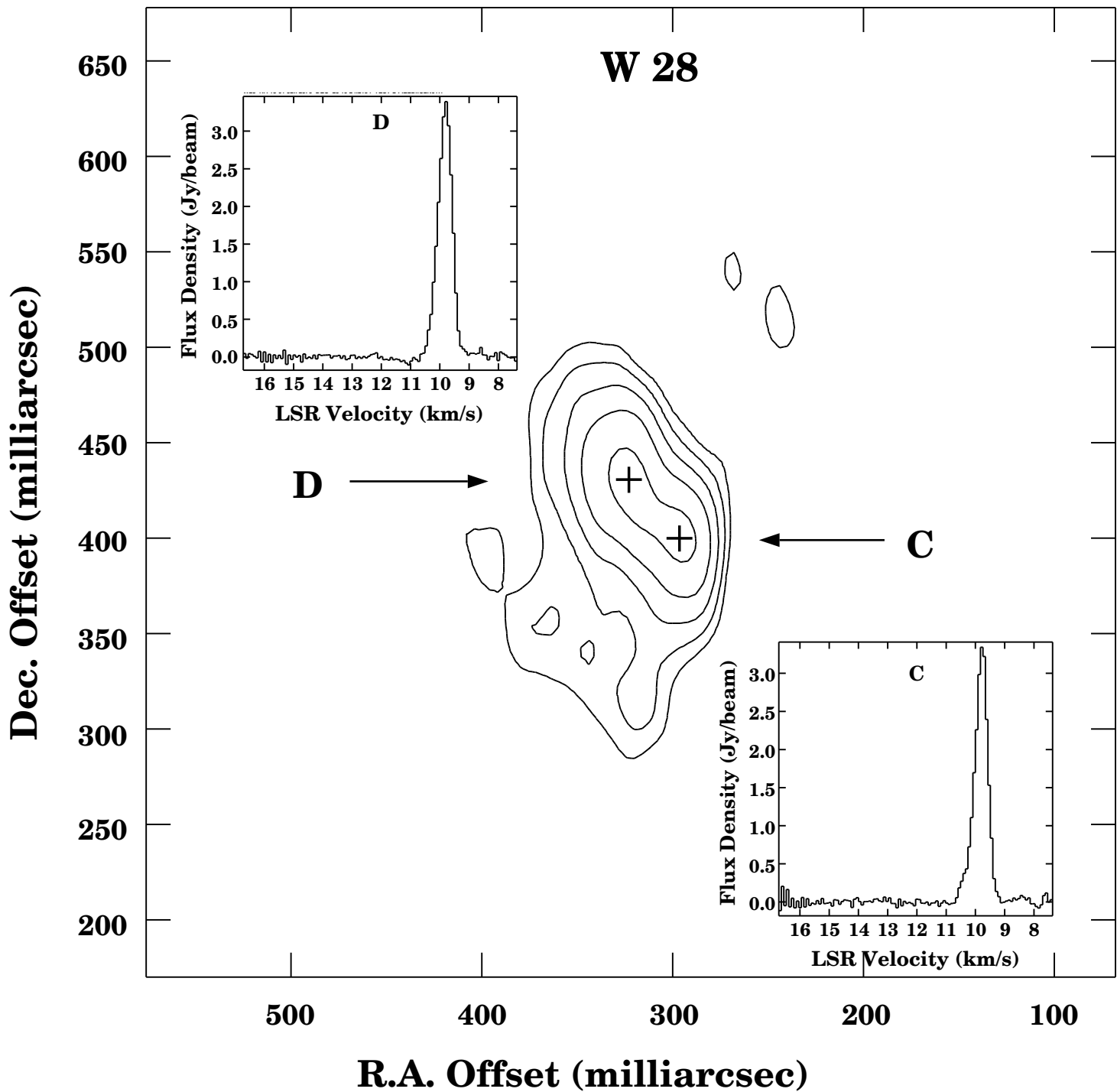
Fig. 3.— (a) For the W 28 position marked **B** from Figure 1, the Stokes *V* profile (solid line) and the derivative of the Stokes *I* profile, scaled by +2.2 milliGauss (line-of-sight field). (b) As (a), but for the W 28 position marked **A** from Figure 1. The scaling here is by +1.8 milliGauss (line-of-sight field).

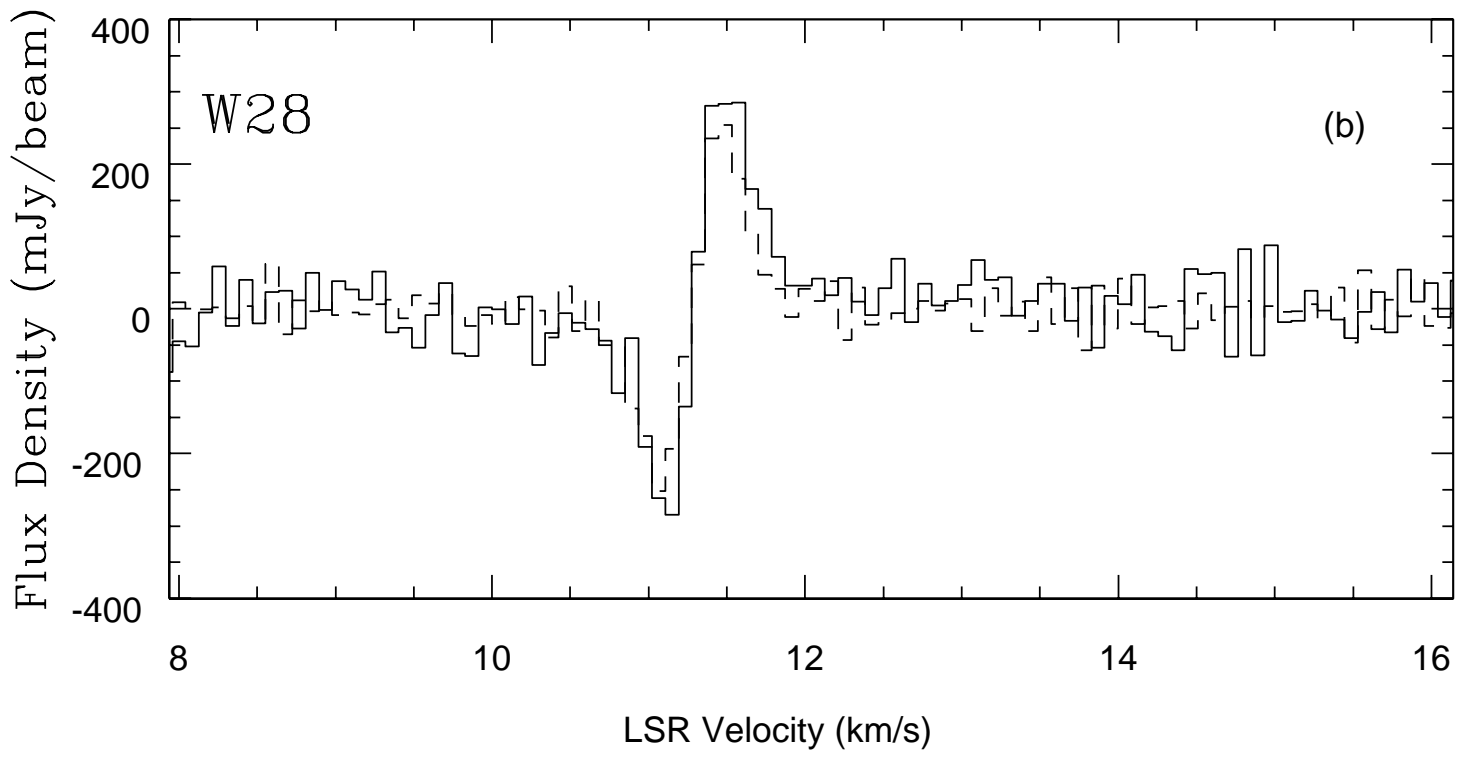
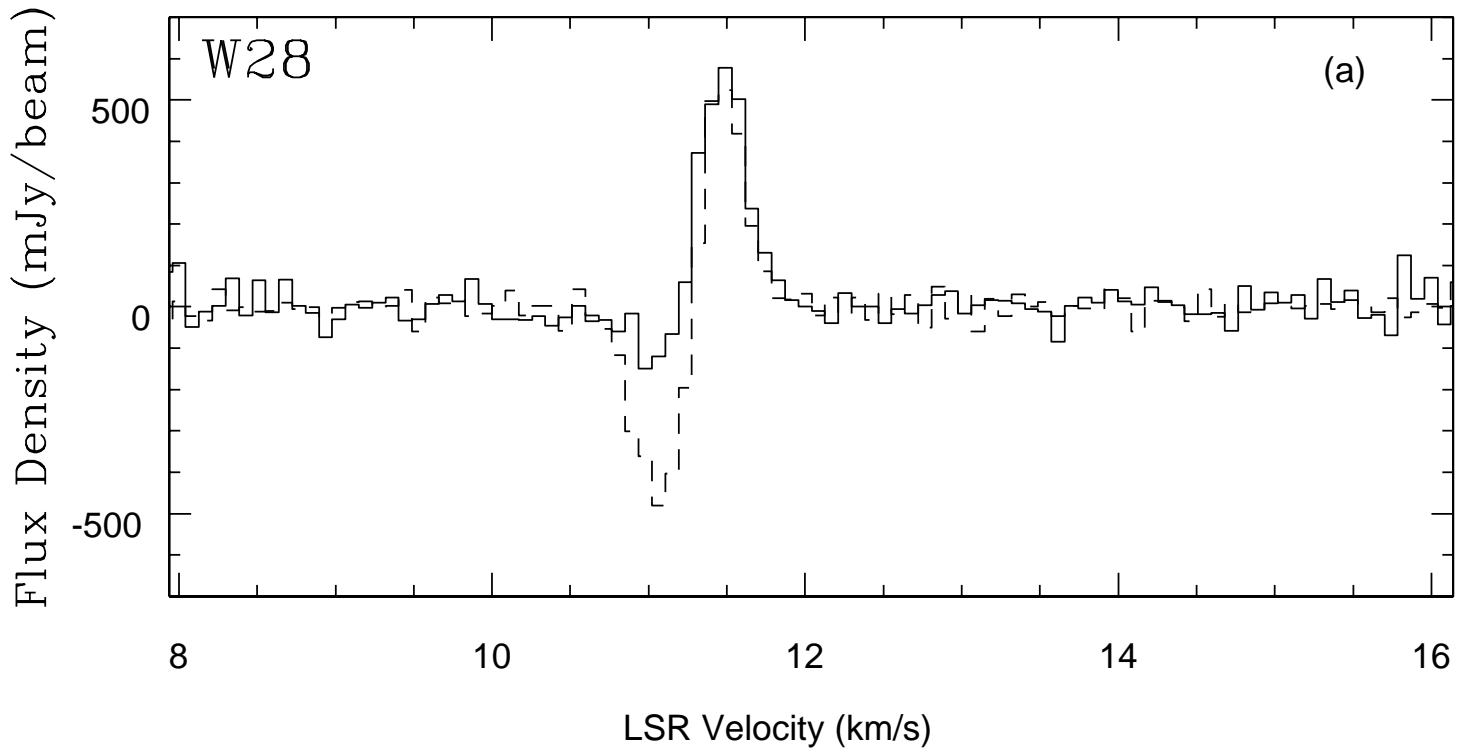
Fig. 4.— A MERLIN contour image of the OH(1720 MHz) maser emission from the W 44 E 11 source. The contours are plotted at -0.05, 0.05, 0.1, 0.2, 0.4, 0.8, 1.6, 3.2 Jy beam⁻¹. The inset shows an OH spectrum taken at the peak in the contour image.

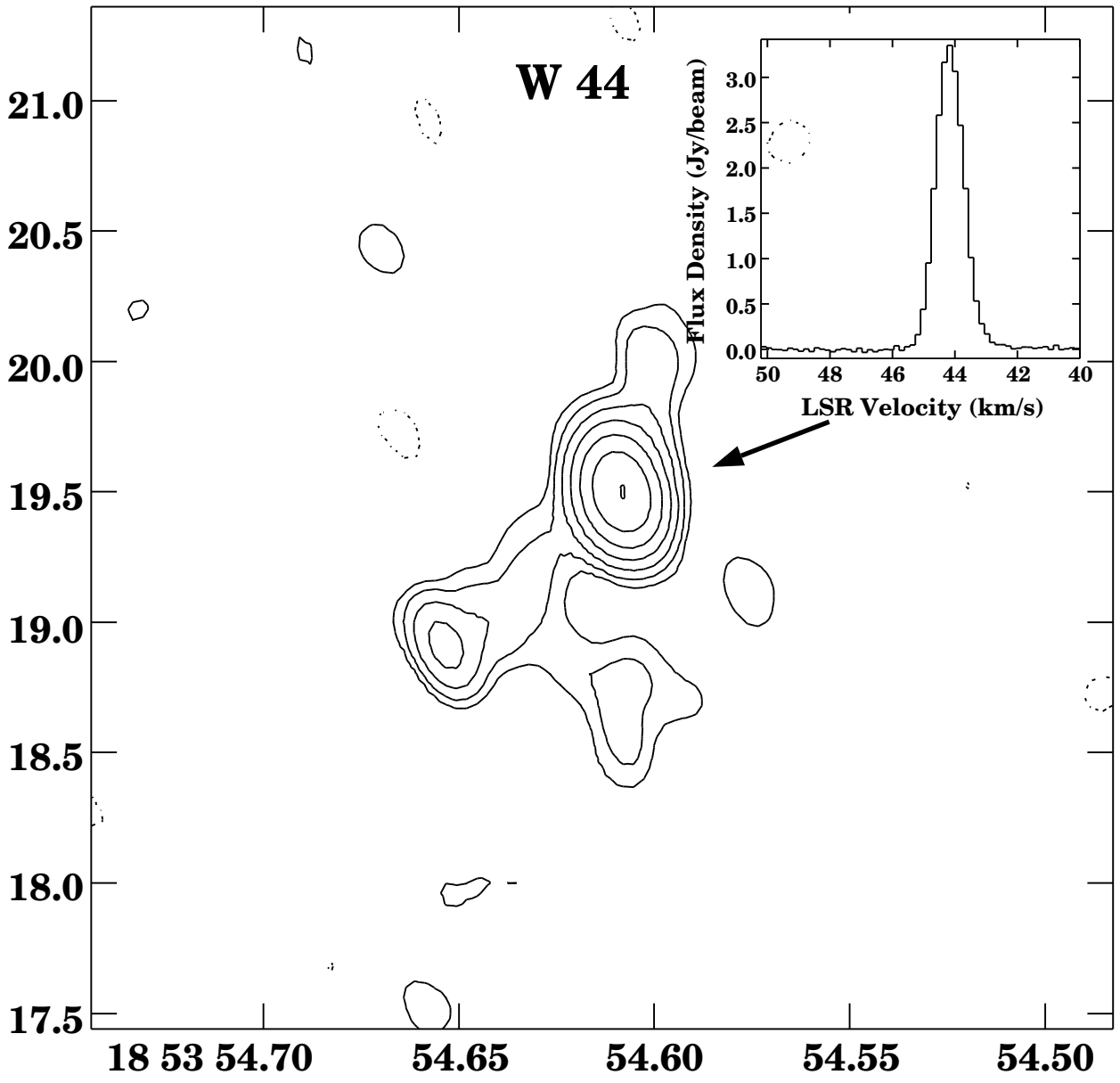
Fig. 5.— A MERLIN contour image of the OH(1720 MHz) maser emission from the W 44 F 24 source. The contours are plotted at -0.075, 0.075, 0.15, 0.3, 0.6, 1.2 Jy beam⁻¹. The inset shows an OH spectrum taken at the peak (marked by a cross) in the contour image.

Fig. 6.— The VLBA contour image of the OH(1720 MHz) maser emission from the W 44 E 11 source.









Declination (B1950)

Right Ascension (B1950)

W 44

Flux Density (Jy/beam)

LSR Velocity (km/s)



